Taylor vortex formation in axial through-flow: Linear and weakly nonlinear analysis

A. Recktenwald and M. Lücke
Institut für Theoretische Physik, Universität des Saarlandes, D-66041 Saarbrücken, Germany

H .W. Müller
Institut für Theoretische Physik, Universität des Saarlandes, D-66041 Saarbrücken, Germany
and Laboratoire de Physique, Ecole Normale Supérieure de Lyon, 46 Allée d'Italie, 69364 Lyon, France
(Received 30 July 1993)

To describe the pattern formation just above the first instability of the rotating Couette-Taylor system in the presence of an externally imposed axial through-flow, an amplitude equation has been derived for the case of a stationary outer cylinder. All linear and nonlinear coefficients of this complex Ginzburg-Landau equation have been calculated numerically and are expressed for a wide range of radius ratios as a function of through-flow strength for small Reynolds numbers. A shooting method has been used to obtain the critical properties of the system. Also, the boundary of the convectively unstable regime has been determined.

PACS number(s): 47.20.Ky, 47.60.+i, 47.32.−y

I. INTRODUCTION

Open-flow instabilities have always been attracting a lot of research activities. For an introduction and examples see [1–4]. Recently there has been an increasing interest in those arising as primary instabilities from homogeneous basic states [5–20]. In particular, the Rayleigh-Bénard and rotating Couette-Taylor systems are very attractive examples offering the possibility of well controlled experimental and theoretical conditions to study pattern-forming instabilities in externally tunable flows. In the absence of flow these systems show a forwards bifurcation into a stationary, spatially periodic dissipative structure.

To understand the growth behavior of the secondary flow structure out of perturbations of the basic state in these systems in the presence of through-flow it was appreciated only recently that one has to distinguish [5,14–16,21–23] three regions [(i)–(iii), cf. below] in the control parameter plane spanned by the through-flow rate and the driving strength. Müller *et al.* [5] have discussed the necessity of this distinction for understanding convection in the Rayleigh-Bénard system subject to a horizontal Poiseuille flow. They have determined the boundaries of the regions while Babcock *et al.* [14] determined them for the Couette-Taylor system. The regions are classified by the spatiotemporal behavior of different *infinitesimal* deviations from the basic homogeneous flow state, i.e., the classification [1,24–26] is based on a linear analysis, as follows.

(i) In the absolutely stable regime any perturbation — spatially localized as well as extended — decays. Region (i) is located in the control parameter plane at small driving. Its boundary can be computed by standard growth analysis of plane wave perturbations.

(ii) In the convectively unstable regime a spatially localized perturbation with an envelope decaying to zero cannot propagate upstream. While being advected downstream it can grow but eventually is blown out of the system. Thus, in the absence of a permanent source of perturbations the system returns to the basic state everywhere. However, a persistently operating source of perturbations that emits $\omega - k$ modes which can grow will generate downstream from its location a source-sustained secondary flow structure [21]. This source-sustained flow pattern reflects and sensitively depends on the source properties. In the control parameter plane the convectively unstable regime is located at larger driving and smaller through-flow than region (i). The boundary between (i) and (ii) is determined by a particular saddle point in the complex k plane of the dispersion of infinitesimal perturbations of the basic state.

(iii) In the absolutely unstable regime a spatially localized perturbation grows and expands in the downstream as well as in the upstream direction. Thus, on the boundary between (ii) and (iii) the upstream facing front of the localized perturbation is stationary in the laboratory frame. Or, equivalently, the upstream front velocity in a frame comoving with the wave packet is equal in size to the packet's downstream group velocity. The growth of the secondary flow structure in region (iii) continues until nonlinear saturation occurs. Then a final nonlinear flow state is reached where — for not too large driving and through-flow — rotationally symmetric Taylor vortices or convective rolls, respectively, are propagating downstream under a stationary intensity envelope. Structural and dynamical properties of this nonlinear state, e.g., the streamwise profiles of intensity, wave number, and phase velocity and the frequency seem to be uniquely selected and seem to depend only weakly on boundary conditions at the inlet or outlet and on perturbations [5,14,16,27].

The Couette-Taylor setup [28] is besides the Rayleigh-Bénard system a prototype example for studying forwards bifurcating, stationary, spatially periodic dissipative structures. Small-amplitude expansions around the threshold (i) of linear stability lead to Ginzburg-Landau equations [29–32] which provide an appropriate quantita-

tive description of the properties of the primary patterns in the weakly nonlinear domain. Therefore we found it worthwhile to derive the complex Ginzburg-Landau equation for rotationally symmetric Taylor vortices in axial through-flow in close analogy to previous work on the Bénard system [5].

The Couette-Taylor system with axial through-flow has been the subject of research ever since the early theoretical [33] and experimental work [34,35]. In particular, the stability behavior of the basic state has attracted theoretical [14,19,36–44] and experimental [13–20,45–48] interest. Historically, the first theoretical stability analyses were based on various approximations such as, e.g., simplified axial through-flow profiles [36–38,42] or the narrow-gap limit [39–41]. Furthermore, prior to 1989 the significance of the convectively unstable regime in the Couette-Taylor system was not generally appreciated. In fact, Tagg *et al.* [22] used this concept in the Couette-Taylor system first without through-flow for counterrotating cylinders. Also the earlier experiments [13,17–20,45–48] did not distinguish between convectively and absolutely unstable regimes so that deviations from theoretical results are not surprising. Only recently theoretical [23] and experimental [14–16] investigations have addressed the problem that the convectively unstable Couette-Taylor system with through-flow acts as a selective amplifier [21] of perturbations and noise.

In this work we present all the theoretical quantities that are needed for a quantitative linear and weakly nonlinear description of the spatiotemporal properties of Taylor vortices in axial through-flow. For the critical quantities as well as for all linear and nonlinear coefficients of the amplitude equation we provide fit formulas covering through-flow rates up to $Re = 20$ and a wide range of radius ratios, η, of the rotating cylinders.

After describing the system in Sec. II we present in Sec. III the results of a linear stability analysis of the basic state against axisymmetric perturbations. The computation is done numerically by means of a shooting method for $0.1 \leq \eta < 1$ and $0 \leq Re \leq 20$. The weakly nonlinear analysis presented in Sec. IV leads to a complex Ginzburg–Landau equation which governs the spatiotemporal evolution of the envelope of the most unstable mode. Details of this derivation are outlined in the Appendix. The actual results, i.e., the numerical values of the coefficients, are compiled in Tables I and II.

II. THE SYSTEM

We consider the axisymmetric flow of an incompressible fluid in the annulus between two concentric cylinders of inner radius r_1 and outer radius r_2 with a gap width $d = r_2 - r_1$ [28,49]. The restriction to axisymmetric flow is justified by experiments for weak through-flow [14–20]. With infinitely long cylinders the only relevant parameter characterizing the geometry is the radius ratio $\eta = r_1/r_2$. The outer cylinder is at rest while the inner one rotates with constant rate Ω. We use the Taylor number

$$T = \frac{1-\eta}{\eta}\left(\frac{\Omega\, r_1 d}{\nu}\right)^2 \tag{2.1}$$

to measure the driving, where ν is the kinematic viscosity. Furthermore, in our system there is an externally imposed axial flow measured by the axial Reynolds number

$$Re = \frac{\bar{w} d}{\nu}\,. \tag{2.2}$$

The mean axial velocity $\bar{w}$, averaged over the annular cross section, is in our parameter range independent of time and axial position and given by the total through-flow.

We also use the relative control parameters

$$\mu = \frac{T}{T_c(Re)} - 1, \quad \epsilon = \frac{T}{T_c(Re=0)} - 1, \tag{2.3}$$

measuring the distances from the critical Taylor numbers, T_c, for onset of Taylor vortices in the presence ($Re \neq 0$) and in the absence ($Re = 0$) of through-flow, respectively. In this notation

$$\epsilon_c(Re) = \frac{T_c(Re)}{T_c(Re=0)} - 1 \tag{2.4}$$

is the reduced, Re dependent critical threshold for onset of vortex flow, i.e., the boundary between regions (i) and (ii) described in the Introduction.

In the absolutely stable regime (i) below the stability boundary $\epsilon_c(Re)$ the flow field $\mathbf{U}(r)$ is rotationally symmetric, axially homogeneous, and constant in time. It consists of a linear superposition of circular Couette flow (CCF) in azimuthal direction, $\mathbf{e}_\varphi$, and of annular Poiseuille flow (APF) in axial direction, $\mathbf{e}_z$,

$$\mathbf{U}(r) = V_{\mathrm{CCF}}(r)\mathbf{e}_\varphi + W_{\mathrm{APF}}(r)\mathbf{e}_z \tag{2.5}$$

without any radial component. Here

$$V_{\mathrm{CCF}}(r) = A\, r + B/r \tag{2.6}$$

with $A = -\frac{\eta}{(1+\eta)}$ and $B = \frac{\eta}{(1-\eta)(1-\eta^2)}$, while

$$W_{\mathrm{APF}}(r) = \frac{r^2 + C\,\ln\, r + D}{E} Re \tag{2.7}$$

with $C = \frac{1+\eta}{(1-\eta)}\frac{1}{\ln\eta}$, $D = \frac{1+\eta}{(1-\eta)}\frac{\ln(1-\eta)}{\ln\eta} - \frac{1}{(1-\eta)^2}$, $E = -\frac{1}{2}[1 + \frac{1}{1-\eta}(\frac{2\eta}{1-\eta} + \frac{1+\eta}{\ln(\eta)})]$. Here and in the following we scale positions by the gap width d, time by the radial momentum diffusion time d^2/ν, azimuthal velocities by the rotational velocity of the inner cylinder $\Omega\, r_1$, and radial and axial velocities by ν/d. The radial profiles of CCF and APF are presented for different radius ratios in Fig. 1.

At the stability threshold $\epsilon_c(Re)$ to be determined in the next section, the basic flow state (2.5) becomes unstable against axially extended perturbations. A stable nonlinear solution of rotationally symmetric Taylor vortices propagating in the downstream direction branches off the basic solution (2.5) of the Navier-Stokes equations. We take the axisymmetric deviation

$$\mathbf{u}(r,z;t) = u\,\mathbf{e}_r + v\,\mathbf{e}_\varphi + w\,\mathbf{e}_z \tag{2.8}$$

of the velocity field from the basic flow (2.5) as the order parameter field to characterize the secondary flow structure. Furthermore, we define auxiliary fields [19,50]

$$x = \left(\partial_r + \frac{1}{r}\right) u - p \ , \tag{2.9a}$$

$$y = \left(\partial_r + \frac{1}{r}\right) v \ , \tag{2.9b}$$

$$\tilde{z} = \partial_r w \ , \tag{2.9c}$$

all depending on r, z, t. They are introduced to eliminate the pressure p and to transform the Navier-Stokes equations into a system of six coupled equations being of first order in ∂_r

$$\mathcal{L}\vec{Y} = \vec{N} \tag{2.10a}$$

for the vector $\vec{Y}$

$$\vec{Y}(r,z,t) = (u,v,w,x,y,\tilde{z})^T. \tag{2.10b}$$

Having only first order radial derivatives is necessary for solving the linear equations $\mathcal{L}\vec{Y} = \vec{0}$ by a shooting method in Sec. III.

The linear operator $\mathcal{L}$ is given by

$$\mathcal{L} = \begin{pmatrix} -\partial_r - \frac{1}{r} & 0 & -\partial_z & 0 & 0 & 0 \\ 0 & -\partial_r - \frac{1}{r} & 0 & 0 & 1 & 0 \\ 0 & 0 & -\partial_r & 0 & 0 & 1 \\ L & -2\frac{\eta}{1-\eta} T \frac{V_{\mathrm{CCF}}}{r} & 0 & -\partial_r & 0 & 0 \\ (\partial_r + \frac{1}{r}) V_{\mathrm{CCF}} & L & 0 & 0 & -\partial_r & 0 \\ \partial_r W_{\mathrm{APF}} & 0 & L - \partial_z^2 & -\partial_z & 0 & -\partial_r - \frac{1}{r} \end{pmatrix}, \tag{2.10c}$$

where

$$L = \partial_t - \partial_z^2 + W_{\mathrm{APF}} \partial_z \tag{2.10d}$$

contains the time derivative. Note that the first row of $\mathcal{L}$ reflects the incompressibility condition $(\partial_r + 1/r)u + \partial_z w = 0$, the second and third one relate y and $\tilde{z}$ to v and w, respectively, and the last three rows contain the linear parts of the Navier-Stokes equations for u, v, w. The nonlinear part of (2.10a) is

$$\vec{N} = \left(0,0,0, u\partial_z w - w\partial_z u + \frac{u^2 + \frac{\eta}{1-\eta} T v^2}{r}, -uy - w\partial_z v, -uz - w\partial_z w\right)^T. \tag{2.11}$$

Equations (2.10) have to be solved subject to the boundary conditions $u = v = w = 0$ at the inner and outer cylinder.

III. LINEAR STABILITY ANALYSIS

In this section we present the results of a numerical stability analysis of the basic flow state against axially extended and localized perturbations. Restricting ourselves to small through-flow, $0 \le Re \le 20$, we consider only axisymmetric perturbations in the range $0.1 \le \eta < 1$ of radius ratios. Note, however, that for the larger η values the growth threshold for nonaxisymmetric disturbances lies, e.g., for $Re = 0$, just above that one for axisymmetric perturbations [51,52].

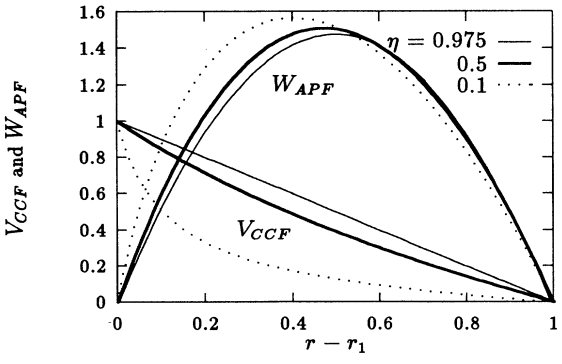

FIG. 1. Radial profiles of the circular Couette flow, $V_{\mathrm{CCF}}(r)$, and annular Poiseuille flow, $W_{\mathrm{APF}}(r)$, defining the basic state for different radius ratios η.

A. The problem

We solve the linear problem

$$\mathcal{L}\vec{Y} = \vec{0} \tag{3.1a}$$

with $\mathcal{L}$ given by (2.10c), (2.10d) with the ansatz

$$\vec{Y}(r,z,t) = \vec{\hat{Y}}(r) e^{ikz+st} + \text{c.c.}, \qquad s = \sigma - i\omega. \tag{3.1b}$$

Here k is the axial wave number of the perturbation. The real part $\sigma = \mathrm{Re}(s)$ of the complex characteristic exponent is the growth rate of the perturbation while $\omega = -\mathrm{Im}(s)$ characterizes its oscillation frequency. $\vec{\hat{Y}}(r)$ is a complex amplitude function. Equations (3.1) are a linear eigenvalue problem with the boundary requirements on the eigenfunction $\vec{\hat{Y}}(r)$ making the eigenvalue spectrum discrete. The eigenvalues s are functions of the

parameters k, T, Re, η appearing in the equations. We are here interested only in the dispersion relation $s(k, T, Re, \eta)$ of that eigenvalue with the largest real part σ. This eigenvalue characterizes the most dangerous perturbation of the basic state, i.e., that one with the largest growth rate. In our system this eigenvalue is simple, i.e., nondegenerate.

To solve the eigenvalue problem we used a standard shooting method [53–55]. Therein the system of 6×6 ordinary differential equations for $\vec{Y}(r)$ is integrated by a fourth order Runge-Kutta method from r_1 to r_2 starting at r_1 with $u = v = w = 0$. This is actually done three times with three different linearly independent "initial" conditions on x, y, $\tilde{z}$. The resulting three fundamental vectors $\vec{Y}(r)$ can be linearly combined to the eigenvector that satisfies the required boundary condition on u, v, w at the upper integration end r_2. This gives rise to a solvability condition — the complex determinant of the 3×3 matrix consisting of u, v, w at r_2 from the three "shots" has to vanish — which in turn determines $s(k, T, Re, \eta)$. To that end we used a two-dimensional Newton-Raphson algorithm with a Richardson extrapolation based on Runge-Kutta step sizes $h_1 = 0.01$ and $h_2 = 0.005$.

The complex dispersion s and the associated eigenvector $\vec{Y}(r)$ contain all the relevant information on the linear spatiotemporal behavior of small perturbations. The condition $\sigma = \mathrm{Re}\ s = 0$ corresponds to neutral stability and determines the neutral curve $T_{\mathrm{stab}}(k, Re, \eta)$ above which an axially extended, axisymmetric perturbation $\sim e^{ikz}$ can grow. The minimum of the curve of $T_{\mathrm{stab}}(k, Re, \eta)$ versus k gives the critical Taylor number $T_c(Re, \eta)$ and the critical wave number $k_c(Re, \eta)$ and the corresponding critical frequency $\omega_c(Re, \eta) = -\mathrm{Im}\ s(k_c, T_c, Re, \eta)$.

B. The critical values

We have evaluated the critical values for many radius ratios in the range $0.1 \leq \eta < 1$ and we have fitted for each η the Re dependence by a power law expansion in Re that represents our data quite well in the range $0 \leq Re \leq 20$. The coefficients of these expansions are presented in Tables I and II. The expansions are based on the following symmetry properties of the system: When reversing the through-flow direction the growth rate σ of perturbations remains unchanged while the phase velocity ω/k of the downstream propagating disturbance wave changes its direction. Thus σ and with it T_c is for fixed k an even function of Re whereas ω is odd. For small Re one finds that T_c and k_c grow quadratically with Re, albeit with different curvature, so that axial through-flow stabilizes the basic state. On the other hand, ω_c varies linearly with Re and vanishes at $Re = 0$. The η dependence of the expansion coefficients presented in Tables I and II is generally stronger at small η than at large η.

As far as possible we have compared our results with those available in the literature: We have reproduced the highly accurate $Re = 0$ critical data of Dominguez-Lerma *et al.* [56] for $0.1 \leq \eta \leq 0.975$ with the same accuracy. With through-flow we confirm results of Takeuchi and Jankowski [19] for $\eta = 0.5$. These results differ from those of Chung and Astill [44] and of Hasoon and Martin [42] which demonstrates that the use of an averaged axial velocity profile [42] causes errors. Finally we reproduced the $\eta = 0.738$ through-flow results of Babcock *et al.* [14].

C. Boundary between convectively and absolutely unstable regime

The knowledge of the complex dispersion relation $s(k, T, Re, \eta)$ allows us not only to determine the critical threshold T_c, i.e., the border between region (i) and (ii) as discussed in the Introduction but also T^c_{conv}, the boundary between the convectively unstable region (ii) and the absolutely unstable region (iii). T^c_{conv} is given by the condition [1,24–26]

$$\mathrm{Re}\ s(\kappa, T) = 0, \tag{3.2a}$$

where $\kappa(T)$ is the saddle position of $s(k, T)$ determined by solving

$$\frac{\partial\, s(\kappa, T)}{\partial\, \kappa} = 0 \tag{3.2b}$$

in the complex k plane. Here we do not display the dependence on Re, η to avoid clumsiness.

We have determined T^c_{conv} or equivalently

$$\mu^c_{\mathrm{conv}} = \frac{T^c_{\mathrm{conv}}}{T_c} - 1, \quad \epsilon^c_{\mathrm{conv}} = \epsilon_c + (1 + \epsilon_c)\mu^c_{\mathrm{conv}}\ , \tag{3.3}$$

for small $\mu^c_{\mathrm{conv}} \ll 1$ by expanding the dispersion relation around the critical point k_c, T_c for fixed Re, η:

$$s(k, T) = s_c + (k - k_c)\left(\frac{\partial s}{\partial k}\right)_c + \frac{1}{2}(k - k_c)^2\left(\frac{\partial^2 s}{\partial k^2}\right)_c + (T - T_c)\left(\frac{\partial s}{\partial T}\right)_c + \text{h.o.t.}, \tag{3.4}$$

where h.o.t. denotes the higher-order terms. From the neutral stability curve $T_c(k)$ it follows that for slightly supercritical drive, $0 \leq \mu \ll 1$, only wave numbers out of a band of width $k - k_c \sim \sqrt{\mu}$ can grow. Hence h.o.t. in (3.4) effectively covers terms at least of order $\mu^{\frac{3}{2}}$. Thus T^c_{conv} resulting from (3.4) can be expected to be a good approximation of the exact boundary (as obtained, e.g., by Babcock *et al.* [14] for $\eta = 0.738$) only for small μ^c_{conv}.

The saddle of (3.4) lies at

$$\kappa = k_c - \frac{(\partial s/\partial k)_c}{(\partial^2 s/\partial k^2)_c} \tag{3.5}$$

and T^c_{conv} then follows from (3.2a)

$$0 = \mathrm{Re}\left[(T - T_c)\left(\frac{\partial s}{\partial T}\right)_c - \frac{1}{2}\frac{(\partial s/\partial k)^2_c}{(\partial^2 s/\partial k^2)_c}\right]\ . \tag{3.6}$$

TABLE I. Even critical values and coefficients of the amplitude equation for different η. The coefficients have been fitted in the range $0 \leq Re \leq 20$. Terms marked by $*$ contribute with a different sign. γ depends on the normalization of the critical linear eigenfunction $\hat{u}(r)$ (4.1). We used $|\hat{u}(r = r_1 + 0.5)| = 15.2$.

Coefficients \ η	0.1	0.2	0.3	0.4	0.5	0.6	0.7	0.738	0.75	0.8	0.9	0.975
					$T_c = a_0[1 + (Re/a_2)^2 + (Re/a_4)^4]$							
a_0	177644	31073.6	12510.4	6996.58	4649.33	3428.73	2708.02	2509.08	2452.51	2243.59	1924.69	1746
a_2	43.81	40.2	38.42	37.43	36.82	36.45	36.22	36.16	36.14	36.08	36.00	35.97
a_4	103.9	74.23	69.26	67.23	66.24	65.71	65.45	65.39	65.37	65.33	65.31	65.34
					$k_c = a_0[1 + (Re/a_2)^2 - (Re/a_4)^4]$							
a_0	3.3393	3.2632	3.2149	3.1835	3.1625	3.1483	3.1389	3.1362	3.1354	3.1326	3.1288	3.127
a_2	133.1*	866.4	269.8	213	191	180.3	175	173.9	173.6	172.8	172.6	173.5
a_4	74.76*	152.8	118.5	114.4	114.9	116.9	119.4	120.4	120.8	122.1	124.8	126.9
					$\xi_0^2 = a_0[1 - (Re/a_2)^2 + (Re/a_4)^4]$							
a_0	0.123	0.131	0.136	0.14	0.142	0.144	0.145	0.145	0.145	0.145	0.146	0.146
a_2	53.9	47	43.4	41.4	40.2	39.5	39.1	39	39	38.9	38.8	38.8
a_4	55.3	48	44.9	43.2	42.3	41.7	41.4	41.3	41.3	41.2	41.2	41.2
					$\tau_0 = a_0[1 - (Re/a_2)^2 + (Re/a_4)^4]$							
a_0	0.0651	0.069	0.0716	0.0733	0.0744	0.0752	0.0757	0.0759	0.0759	0.0761	0.0763	0.0764
a_2	48.6	44.8	42.6	41.3	40.5	40	39.7	39.7	39.6	39.6	39.5	39.4
a_4	49.7	47.1	45.4	44.3	43.7	43.3	43	43	43	42.9	42.8	42.8
					$\epsilon_c^{\mathrm{conv}} = (Re/a_2)^2 + (Re/a_4)^4$							
a_2	7.96	8.01	8.	7.99	7.98	7.97	7.96	7.96	7.96	7.96	7.95	7.95
a_4	22.5	21.4	20.7	20.2	19.9	19.7	19.6	19.6	19.6	19.5	19.5	19.5
					$\gamma = a_0[1 - (Re/a_2)^2 + (Re/a_4)^4]$							
a_0	11.2	10.9	10.6	10.1	9.48	8.84	8.17	7.92	7.84	7.5	6.83	6.34
a_2	38.7	36.4	35.5	35.1	35	35.1	35.5	35.6	35.7	35.9	36.6	37.2
a_4	43	40.2	39.2	38.8	38.8	38.9	39.3	39.5	39.5	39.8	40.6	41.3

TABLE II. Odd critical values and coefficients of the amplitude equation for different η. The coefficients have been fitted in the range $0 \leq Re \leq 20$. Terms marked by $*$ contribute with a different sign.

Coefficients \ η	0.1	0.2	0.3	0.4	0.5	0.6	0.7	0.738	0.75	0.8	0.9	0.975
					$\omega_c = a_1 Re[1 + (Re/a_3)^2]$							
a_1	4.236	3.994	3.863	3.784	3.735	3.703	3.682	3.676	3.675	3.669	3.661	3.658
a_3	258.1*	420.0*	529.9	307.4	254.1	231.3	220.3	217.9	217.2	215.4	214.3	215.3
					$v_g = a_1 Re[1 + (Re/a_3)^2]$							
a_1	1.33	1.28	1.26	1.25	1.24	1.23	1.23	1.23	1.23	1.23	1.23	1.23
a_3	459	732	748	652	576	527	495	486	484	475	461	453
					$c_0 = (Re/a_1)[1 - (Re/a_3)^2]$							
a_1	282	185	160	149	144	140	139	139	138	138	138	138
a_3	145	66.9	59.4	56	54.1	52.9	52.1	51.9	51.8	51.6	51.2	51.0
					$c_1 = (Re/a_1)[1 + (Re/a_3)^2]$							
a_1	60	50.6	46.1	43.7	42.3	41.4	40.9	40.8	40.7	40.6	40.5	40.4
a_3	90.5	85.9	80.2	76.4	73.8	72.1	71	70.6	70.5	70.2	69.6	69.3
					$c_2 = (Re/a_1)[1 - (Re/a_3)^2]$							
a_1	-79.9	-144	-251	-527	-4990	762	362	302	287	237	173	143
a_3	53.1	47.7	40.4	31.5	12.2	42.3*	322*	111	97.8	73.3	57.6	52.3

Using the data from our shooting method we have evaluated numerically the derivatives entering (3.6). The results are displayed in Tables I and II. There we have represented the derivatives in terms of the quantities that enter also the amplitude equation (see below)

$$\left(\frac{\partial s}{\partial k}\right)_c = -i\left(\frac{\partial \omega}{\partial k}\right)_c = -i\, v_g, \tag{3.7a}$$

$$\left(\frac{\partial s}{\partial T}\right)_c = \left(\frac{\partial \sigma}{\partial T}\right)_c - i\left(\frac{\partial \omega}{\partial T}\right)_c = \frac{1+ic_0}{\tau_0 T_c}, \tag{3.7b}$$

$$\left(\frac{\partial^2 s}{\partial k^2}\right)_c = \left(\frac{\partial^2 \sigma}{\partial k^2}\right)_c - i\left(\frac{\partial^2 \omega}{\partial k^2}\right)_c = -\frac{2\,\xi_0^2}{\tau_0}(1+i\,c_1). \tag{3.7c}$$

Here v_g is the critical group velocity, $1/\tau_0 = T_c(\partial\sigma/\partial T)_c$ measures the linear increase of the growth rate with μ, $\xi_0^2 = \frac{1}{2T_c}\left(\frac{d^2 T_{\rm stab}(k)}{dk^2}\right)_c$ is the curvature of the neutral stability curve at its minimum, $c_0 = -\tau_0 T_c(\partial\omega/\partial T)_c$ and $c_1 = \frac{\tau_0}{2\xi_0^2}\left(\frac{\partial^2\omega}{\partial k^2}\right)_c$. In (3.7c) we have used the relation [57]

$$\left(\frac{\partial^2 \sigma}{\partial k^2}\right)_c = -\left(\frac{\partial \sigma}{\partial T}\frac{d^2 T_{\rm stab}(k)}{dk^2}\right)_c \tag{3.8}$$

to relate the second k derivative of the growth rate to the critical curvature ξ_0^2. Inserting the expressions (3.7) into (3.6) one finds the boundary between the convectively and absolutely unstable regions

$$\mu^c_{\rm conv} = \frac{v_g^2 \tau_0^2}{4\xi_0^2(1+c_1^2)} \tag{3.9}$$

[1,5,21,22,58]. The Re, η dependence of the quantities entering (3.9) as well as that of $\mu^c_{\rm conv}$ can be seen from the tables. For small through-flow τ_0, ξ_0 — being derivatives of σ — vary $\sim Re^2$ whereas v_g, c_0, c_1 — being derivatives of ω — vary $\sim Re$ so that $\mu^c_{\rm conv}$ grows $\sim Re^2$. Figure 2 shows $\epsilon^c_{\rm conv}$ according to (3.3) and ϵ_c as a function of Re.

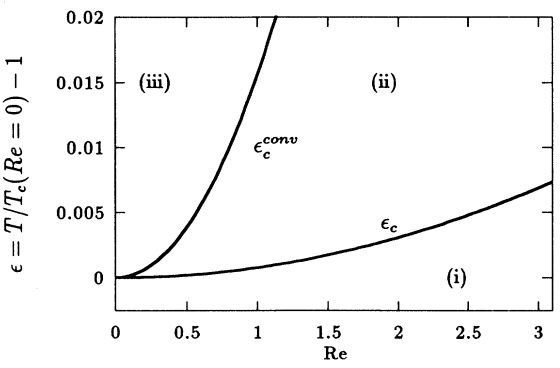

FIG. 2. Convective vs absolute instability for axisymmetric perturbations. The basic flow state is absolutely stable in the region (i) below the curve ϵ_c, convectively unstable in the region (ii) between the curves $\epsilon^c_{\rm conv}$ and ϵ_c, and absolutely instable in the region (iii) above the curve $\epsilon^c_{\rm conv}$. Here the radius ratio is $\eta = 0.75$ but the curves practically do not vary with η in the plot range shown.

IV. WEAKLY NONLINEAR ANALYSIS: AMPLITUDE EQUATION

Close above the threshold of linear stability the critical mode saturates and the nonlinear state can be described by

$$\vec{Y}(r,z,t) = (u,v,w,x,y,\tilde{z})^T = A(z,t)\vec{Y}(r)e^{i(k_c z-\omega_c t)} + \text{c.c.} \tag{4.1}$$

The fields (4.1) describe a downstream propagating Taylor vortex pattern that in the absence of through-flow would be stationary. $\vec{Y}(r)$ is the complex eigenvector of the linear problem (3.1) at T_c. An upstream traveling wave does not appear in (4.1) since only one eigenvalue of (3.1) becomes critical. $A(z,t)$ is the saturation amplitude determined by the nonlinearity in the field equations. For slightly supercritical driving ($0 \le \mu \ll 1$) a small band of axial wave numbers with $|k-k_c| \le \sqrt{\mu}$ is excited giving rise to slow spatial and temporal modulations of the vortex structure. To accommodate these variations the complex amplitude A is supposed to vary slowly in z and t. We therefore adopt the method of multiple scales [59] to obtain an amplitude equation from the Navier-Stokes equation. The computation yields a complex Ginzburg-Landau equation of the form

$$\tau_0(\partial_t + v_g\partial_z)A(z,t) = [\mu(1+ic_0) + \xi_0^2(1+ic_1)\partial_z^2 - \gamma(1+ic_2)|A|^2]A(z,t). \tag{4.2}$$

Details of the derivation are outlined in the Appendix. For zero through-flow the Landau equation for a spatially homogeneous Taylor vortex amplitude was determined by Davey [60] and the Ginzburg-Landau equation with spatial derivatives was given by Yahata [32] and Graham and Domaradzki [31].

Since the system is invariant under *simultaneous* reversal of the z coordinate and the through-flow direction the coefficients v_g, c_0, c_1, c_2 are odd while τ_0, ξ_0^2, γ are even functions of Re. This can easily be seen by applying the symmetry transformation ($z \to -z$, $Re \to -Re$, $A \to A^*$) upon Eq. (4.2) and by comparing with the complex conjugate of (4.2). Note that the coefficients v_g, c_0, c_1, c_2 in the amplitude equation appear only for nonzero through-flow, i.e., for propagating Taylor vortices. We have calculated all the coefficients assuming an annulus of infinite axial extension. Best fit formulas for them that are valid up to flow rates $Re = 20$ are given in Tables I and II.

The linear coefficients can be expressed [57] by certain partial derivatives since the linearized amplitude equation reflects the lowest order terms in an expansion of the dispersion $s(k,T,Re,\eta)$ around k_c and T_c for a given

through-flow. But they can be obtained also by special scalar products over eigenfunctions (cf. the Appendix). We calculated them both ways. The deviation between both methods was about 10^{-5}–10^{-4} %. For c_1 it was 10^{-2}%.

$v_g = \left(\frac{\partial\omega}{\partial k}\right)_c$ is the group velocity of the traveling wave at the critical point. It grows almost linearly with Re. The relaxation time τ_0 is defined by $\tau_0^{-1} = T_c \left(\frac{\partial\sigma}{\partial T}\right)_c$. It has a constant value without through-flow and decreases quadratically with Re. The correlation length ξ_0 is given by the curvature of the marginal stability curve, $\xi_0^2 = \frac{1}{2T_c}\left(\frac{\partial^2 T_{\text{stab}}}{\partial k^2}\right)_c$. With through-flow ξ_0^2 decreases which means that the bandwidth of growing modes increases. The coefficient $c_1 = \frac{\tau_0}{2\xi_0^2}\left(\frac{\partial^2\omega}{\partial k^2}\right)_c$ contributing linearly to the dispersion increases linearly with Re as the frequency shift $c_0 = -\tau_0 T_c \left(\frac{\partial\omega}{\partial T}\right)_c$. We reproduced the linear coefficients obtained by Dominguez-Lerma *et al.* [56] without through-flow. Babcock *et al.* [14] did the linear stability analysis for $\eta = 0.738$ in the presence of flow and their results for the linear coefficients are in very good agreement with ours.

We obtained the nonlinear coefficients γ and c_2 by calculating special scalar products of the eigenfunctions (see the Appendix). Note that γ depends on the normalization of the critical eigenvector $\vec{Y}(r)$ of the linear problem. In this work the modulus of the eigenfunction $\hat{u}(r)$, i.e., the first component of $\vec{Y}(r)$, has been normalized to the value of 15.2 in the middle of the gap, $|\hat{u}(r = r_1 + 0.5)| = 15.2$. This scaling allows an easy comparison with the first axial Fourier mode u_1 of the radial velocity field obtained from numerical simulations of the full Navier Stokes equations without through-flow [61,62]. The comparison was based on the small-ϵ extrapolation [61,62] of the scaled numerical Fourier modes $u_1/\sqrt{\epsilon}$. In the presence of a driving ramp extending to subcritical values at one end of the system the numerically obtained u_1 [61] was suppressed by about 1% relative to our amplitude equation result. Simulations with axially periodic boundary conditions, on the other hand, gave $u_1/\sqrt{\epsilon}$ extrapolations that were 0.6% above our result. A comparison with experimental results [63] gave about 0.5% greater value than ours. γ is decreasing quadratically with increasing through-flow. The coefficient c_2 introduces a nonlinear amplitude dependent correction to the phase velocity [cf. Eq. (4.3) below]. It is linear in Re and has to our knowledge not been measured yet.

When boundary influences may be ignored the amplitude equation (4.2) allows a one-parameter family of solutions

$$A(z,t) = F(q)e^{i[qz - \Omega(q)t]}. \tag{4.3a}$$

The modulus

$$F(q) = \sqrt{\frac{\mu - \xi_0^2 q^2}{\gamma}} \tag{4.3b}$$

which is constant in space and time and the frequency

$$\Omega(q) = \frac{1}{\tau_0}[v_g\tau_0 q + \xi_0^2 q^2(c_1 - c_2) - \mu(c_0 - c_2)] \tag{4.3c}$$

depend on the wave number displacement $q = k - k_c$. The solution (4.3) exists for arbitrary $|q| \leq \sqrt{\mu/\xi_0^2}$. However, not all of them are stable, e.g., unstable due to the Eckhaus mechanism. By virtue of (4.1) the solution (4.3a) describes a chain of Taylor vortices with wave number $k = k_c + q$ traveling downstream with a phase velocity $v_{\text{phase}} = [\omega_c + \Omega(q)]/(k_c + q)$. Similar nonlinear behavior can be observed in experiments [14,16] and numerical simulations [5,27] in the absolutely unstable regime (iii) with long cylinders far away from inlet and outlet, where the bulk dynamics is unaffected by the axial boundary conditions. Approaching the ends of the cylinders the structural properties of the propagating vortices are changed at inlet and outlet differently relative to the bulk behavior. Investigations of the effect of various inlet and outlet conditions on A are presented in [5] for the Bénard system and in [27] for the Couette system and will be reported elsewhere.

V. SUMMARY

The Couette-Taylor system subject to an axial through-flow is considered in this article. We have investigated the vicinity of the primary transition from the basic Couette-Poiseuille flow to a downstream traveling chain of axisymmetric Taylor vortices. A complete linear and weakly nonlinear analysis of this structure forming bifurcation is presented for a wide range of radius ratios as a function of the two control parameters, T and Re. Among the various linear properties we have determined in the T-Re plane the boundary $T_c(Re,\eta)$ between the absolutely stable region (i) where no perturbation can grow and the convectively unstable region (ii) as well as the boundary $T^c_{\text{conv}}(Re,\eta)$ between region (ii) and the absolutely unstable region (iii). A nonlinear analysis of the Navier-Stokes equations in the vicinity of the threshold, T_c, for onset of vortex flow leads to an evolution equation for the envelope of the most unstable mode—the amplitude equation. It yields a quantitative linear and weakly nonlinear description of the spatiotemporal dynamics of vortex flow close to the threshold. The numerical values of the linear as well as of the nonlinear coefficients appearing in the amplitude equation are evaluated for a wide range of radius ratios and for flow rates up to $Re = 20$. The results condensed in Tables I and II open the opportunity for further theoretical work and quantitative comparison with experiments and numerical simulations.

ACKNOWLEDGMENTS

Support by the Deutsche Forschungsgemeinschaft and the European Community is gratefully acknowledged.

APPENDIX: DERIVATION OF THE AMPLITUDE EQUATION

The amplitude equation results from a weakly nonlinear perturbation expansion of (2.10) above the threshold

of linear stability. We expand $\mathcal{L}$, $\vec{Y}$, and $\vec{N}$ in powers of $\sqrt{\mu}$. Since for supercritical systems there is a band of k modes that can grow, there will be a slow variation of the critical order parameter fields, which will be expressed by introducing additional slow multiple scales [59] for the space $Z_1 = \mu^{\frac{1}{2}} z$; $Z_2 = \mu z$; ... and for the time $T_1 = \mu^{\frac{1}{2}} t$; $T_2 = \mu t$; ....

Then the partial derivatives become

$$\partial_z \to \partial_z + \mu^{\frac{1}{2}} \partial_{Z_1} + \mu \partial_{Z_2} + \cdots, \tag{A1a}$$

$$\partial_t \to \partial_t + \mu^{\frac{1}{2}} \partial_{T_1} + \mu \partial_{T_2} + \cdots. \tag{A1b}$$

With

$$\vec{Y} = \mu^{\frac{1}{2}} A_0 \vec{Y}_0 + \mu \vec{Y}_1 + + \mu^{\frac{3}{2}} \vec{Y}_2 + \cdots \tag{A2}$$

one has to solve the following set of equations at $\mu = 0$:

$$\mathcal{L}_0 A_0 \vec{Y}_0 = \vec{0}, \qquad O(\mu^{\frac{1}{2}}) \tag{A3a}$$

$$\mathcal{L}_0 \vec{Y}_1 = -\mathcal{L}_1 A_0 \vec{Y}_0 + \vec{N}_1, \qquad O(\mu) \tag{A3b}$$

$$\mathcal{L}_0 \vec{Y}_2 = -\mathcal{L}_1 \vec{Y}_1 - \mathcal{L}_2 A_0 \vec{Y}_0 + \vec{N}_2, \qquad O(\mu^{\frac{3}{2}}). \tag{A3c}$$

Here

$$\mathcal{L}_1 = M_1 \partial_{T_1} + M_2 \partial_{Z_1}, \tag{A3d}$$

$$\mathcal{L}_2 = M_1 \partial_{T_2} + M_2 \partial_{Z_2} + M_3 \partial_{Z_1}^2 + M_4, \tag{A3e}$$

and $M_i = (m_{jk})$ are matrices resulting by inserting (A1) into $\mathcal{L}$ (2.10a). The matrix M_1 is $m_{jk} = 0$ except for $m_{41} = m_{52} = m_{63} = 1$. For M_2 one obtains $m_{jk} = 0$ except for $m_{41} = m_{52} = -2\partial_z + W_{\mathrm{APF}}$, $m_{63} = -4\partial_z + W_{\mathrm{APF}}$, $m_{13} = m_{64} = -1$. M_3 is $m_{jk} = 0$ except for $m_{41} = m_{52} = -1$ and $m_{63} = -2$. $m_{24} = -\frac{2V_{\mathrm{CCF}}}{r}$ is the only nonvanishing element for M_4.

The boundary conditions for $\vec{Y}_0$, $\vec{Y}_1$, and $\vec{Y}_2$ are the same as for $\vec{Y}$ (3.1b) in the linear stability problem. The system (A3) is only solvable if certain conditions are fulfilled. These solvability conditions yield the nonlinear amplitude equation (4.2) for A.

1. Lowest order $\mu^{\frac{1}{2}}$

In this order one has to solve the linear equation at criticality and gets the critical radial eigenvector $\vec{Y}_0$ of the linear stability analysis which was denoted in Sec. II by $\vec{Y}(r)$. For the solvability condition in higher orders we need the adjoint solution. We define a scalar product by

$$\langle \vec{f} \,|\, \vec{g} \rangle := \lim_{\substack{L \to \infty \\ T \to \infty}} \frac{1}{2L} \int_{-L}^{+L} dz \, \frac{1}{2T} \int_{-T}^{+T} dt \int_{r_1}^{r_2} r \, dr \, \vec{f}^* \cdot \vec{g}. \tag{A4}$$

The adjoint operator $\mathcal{L}_0^+$ defined by $\langle \vec{f} | \mathcal{L}_0 \vec{g} \rangle = \langle \mathcal{L}_0^+ \vec{f} | \vec{g} \rangle$ is obtained by transposing $\mathcal{L}_0$ and by replacing ∂_t by $-\partial_t$, ∂_z by $-\partial_z$, and $-\partial_r$ by $\frac{1}{r} + \partial_r$. The adjoint solution defined by $\mathcal{L}_0^+ \vec{Y}_0^+ = 0$ has the form

$$\vec{Y}_0^+(r,z,t) = \hat{\vec{Y}}_0^+(r)\, e^{i(k_c z - \omega_c t)} + \text{c.c.}, \tag{A5}$$

where the adjoint radial eigenfunctions have to fulfill the boundary conditions $x_0^+ = y_0^+ = \tilde{z}_0^+ = 0$ at $r = r_1, r_2$. This follows from the partial integration that leads to the adjoint operator. There the integrated terms have to vanish at the radial boundaries and this can only be fulfilled with the above boundary conditions for the adjoint solutions x_0^+, y_0^+, and $\tilde{z}_0^+$.

2. Order μ

The solvability condition of the inhomogeneous Eq. (A3b) reads

$$0 = \left\langle \vec{Y}_0^+ | \mathcal{L}_0 \vec{Y}_1 \right\rangle = -\left\langle \vec{Y}_0^+ | \mathcal{L}_1 A_0 \vec{Y}_0 \right\rangle + \left\langle \vec{Y}_0^+ | \vec{N}_1 \right\rangle \tag{A6}$$

or explicitly after inserting $\mathcal{L}_1$

$$I_1 \partial_{T_1} A_0 + I_2 \partial_{Z_1} A_0 = 0. \tag{A7}$$

Expressions for the integrals I_1, I_2 are given below. The scalar product with $\vec{N}_1$ vanishes since $\vec{N}_1$ contains only terms of the form $\propto e^0$ and $\propto e^{\pm 2i(k_c z - \omega_c t)}$. Using the solvability condition (A7) in (A3b) one can calculate the radial eigenfunctions $\vec{Y}_1$ numerically. This is done with the ansatz for the eigenfunction

$$\vec{Y}_1 = \partial_{Z_1} A_0 \vec{W} + \vec{Y}_1^{\mathrm{nlin}}, \tag{A8a}$$

where $\vec{W}$ is a function proportional to $e^{\pm i(k_c z - \omega_c t)}$ and

$$\vec{Y}_1^{\mathrm{nlin}} = |A_0|^2 \hat{\vec{Y}}_{10}^{\mathrm{nlin}}(r)\, e^0 + A_0^2 \hat{\vec{Y}}_{12}^{\mathrm{nlin}}(r)\, e^{2i(k_c z - \omega_c t)} + \text{c.c.} \tag{A8b}$$

Note that the contribution (A8b) to $\vec{Y}_1$ comes from the inhomogeneity $\vec{N}_1$. The latter can be divided into two parts, $\vec{N}_{10}\, e^0$ and $\vec{N}_{12}\, e^{\pm 2i(k_c z - \omega_c t)}$. They have the following form:

$$\vec{N}_{10} = 2|A_0|^2 \mathrm{Re} \left[\hat{u}_0 \begin{pmatrix} \vdots \\ -i\, k_c\, \hat{w}_0^* + \dfrac{\hat{u}_0^*}{r} \\ -\hat{y}_0^* \\ -\hat{\tilde{z}}_0^* \end{pmatrix} + i\, k_c\, \hat{w}_0 \begin{pmatrix} \vdots \\ \hat{u}_0^* \\ \hat{v}_0^* \\ \hat{w}_0^* \end{pmatrix} + \frac{\eta}{1-\eta} T_c \begin{pmatrix} \vdots \\ \dfrac{\hat{v}_0\, \hat{v}_0^*}{r} \\ 0 \\ 0 \end{pmatrix} \right] \tag{A9}$$

and

$$\vec{N}_{12} = A_0^2 \left[\hat{u}_0 \begin{pmatrix} \vdots \\ ik_c\hat{w}_0 + \dfrac{\hat{u}_0}{r} \\ -\hat{y}_0 \\ -\hat{\tilde{z}}_0 \end{pmatrix} - ik_c\hat{w}_0 \begin{pmatrix} \vdots \\ \hat{u}_0 \\ \hat{v}_0 \\ \hat{w}_0 \end{pmatrix} + \frac{\eta}{1-\eta} T_c \frac{\hat{v}_0^2}{r} \begin{pmatrix} \vdots \\ 1 \\ 0 \\ 0 \end{pmatrix} \right] + \text{c.c.} \tag{A10}$$

Here the three dots ($\vdots$) denote the first three components being zero.

3. Order $\mu^{\frac{3}{2}}$

We do not have to calculate the solution $\vec{Y}_2$. Equation (A3c) is used only to get from the solvability condition in order $\mu^{\frac{3}{2}}$ the amplitude equation (4.2). The scalar product with the adjoint solution $\vec{Y}_0^+$ yields

$$\underbrace{\left\langle \vec{Y}_0^+ | \mathcal{L}_0 \vec{Y}_2 \right\rangle}_{=0} + \underbrace{\left\langle \vec{Y}_0^+ | \mathcal{L}_1 \vec{Y}_1^{\text{nlin}} \right\rangle}_{=0} + \left[I_1 \partial_{T_2} + I_2 \partial_{Z_2} + \left\langle \vec{Y}_0^+ | M_4 \vec{Y}_0 \right\rangle \right] A_0$$

$$+ \left[\left\langle \vec{Y}_0^+ | M_3 \vec{Y}_0 \right\rangle - \left\langle \vec{Y}_0^+ \middle| \left(\frac{I_2}{I_1} M_1 - M_2 \right) \vec{W} \right\rangle \right] \partial_{Z_1}^2 A_0 - \left\langle \vec{Y}_0^+ | \vec{N}_2 \right\rangle = 0. \tag{A11}$$

The first term vanishes because of the definition of the adjoint solution. The second one vanishes since $\vec{Y}_1^{\text{nlin}}$ contains only terms which, being proportional to e^0 or $e^{\pm 2i(k_c z - \omega_c t)}$, are out of resonance with the critical mode $e^{i(k_c z - \omega_c t)}$ of $\vec{Y}_0^+$. With $A(z,t) = \mu^{\frac{1}{2}} A_0(Z_1, Z_2, \ldots, T_1, T_2) = \mu^{\frac{1}{2}} A_0(z\sqrt{\mu}, \ldots, t\sqrt{\mu})$ we obtain after multiplying the different solvability conditions with their respective μ order and adding them:

$$\left(\partial_t + \frac{I_2}{I_1} \partial_z \right) A = \left(\mu \frac{I_4}{I_1} + \frac{I_w}{I_1} \partial_z^2 - \frac{I_N}{I_1} |A|^2 \right) A, \tag{A12}$$

with

$$\begin{aligned} &I_1 = \left\langle \vec{Y}_0^+ | M_1 \vec{Y}_0 \right\rangle,\ I_2 = \left\langle \vec{Y}_0^+ | M_2 \vec{Y}_0 \right\rangle,\ I_3 = \left\langle \vec{Y}_0^+ | M_3 \vec{Y}_0 \right\rangle,\ I_4 = -\left\langle \vec{Y}_0^+ | M_4 \vec{Y}_0 \right\rangle, \\ &I_w = \left\langle \vec{Y}_0^+ | (\tfrac{I_2}{I_1} M_1 - M_2) \vec{W} \right\rangle - I_3 \text{ and } I_N = -\left\langle \vec{Y}_0^+ | \vec{N}_2 \right\rangle. \end{aligned} \tag{A13}$$

To evaluate I_N we write $\vec{N}_2$ in the form

$$\vec{N}_2 = A_0 |A_0|^2 \, \vec{\hat{N}}_{21} \, e^{i(k_c z - \omega_c t)} + (\text{off-resonant terms}). \tag{A14}$$

Only the first term containing the critical mode $\propto e^{i(k_c z - \omega_c t)}$ contributes to the scalar product I_N. The relevant vector $\vec{\hat{N}}_{21}$ has the form

$$\begin{aligned} \vec{\hat{N}}_{21} = &-\hat{u}_0^* \begin{pmatrix} \vdots \\ -2ik_c\hat{w}_{12} - 2\dfrac{\hat{u}_{12}}{r} - ik_c\hat{w}_{12} \\ \hat{y}_{12} \\ \hat{\tilde{z}}_{12} \end{pmatrix} - ik_c\hat{w}_0^* \begin{pmatrix} \vdots \\ 3\hat{u}_{12} \\ 2\hat{v}_{12} \\ \hat{w}_{12} \end{pmatrix} - \hat{u}_{10} \begin{pmatrix} \vdots \\ -ik_c\hat{w}_0 \\ \hat{y}_0 \\ \hat{\tilde{z}}_0 \end{pmatrix} \\ &-\hat{u}_0 \begin{pmatrix} \vdots \\ -2\dfrac{\hat{u}_{10}}{r} + ik_c\hat{w}_{10} \\ \hat{y}_{10} \\ \hat{\tilde{z}}_{10} \end{pmatrix} - \begin{pmatrix} \vdots \\ -2\frac{\eta}{1-\eta} T_c \dfrac{\hat{v}_0\hat{v}_{10} + \hat{v}_0^*\hat{v}_{12}}{r} \\ \hat{u}_{12}\hat{y}_0^* + ik_c\hat{w}_{10}\hat{v}_0 - ik_c\hat{w}_{12}\hat{v}_0^* \\ \hat{u}_{12}\hat{\tilde{z}}_0^* + ik_c\hat{w}_{10}\hat{w}_0 \end{pmatrix}. \end{aligned} \tag{A15}$$

Rearranging Eq. (A12) we get the amplitude equation (4.2) where the coefficients are expressed by special scalar products:

$$\frac{1}{\tau_0}(1 + ic_0) = \frac{I_4}{I_1}, \qquad \frac{\xi_0^2}{\tau_0}(1 + ic_1) = \frac{I_w}{I_1},$$

$$\frac{\gamma}{\tau_0}(1 + ic_2) = \frac{I_N}{I_1}.$$

[1] P. Huerre, in *Instabilities and Nonequilibrium Structures*, edited by E. Tirapegui and D. Villaroel (Reidel, Dordrecht, 1987), p. 141; P. Huerre and P. A. Monkewitz, Annu. Rev. Fluid Mech. **22**, 473 (1990).

[2] An early review of the Rayleigh-Bénard system with shear flow is given by R. E. Kelly, in *The Onset and Development of Rayleigh-Bénard Convection in Shear Flows*, Proceedings of the International Conference on Physical Chemistry and Hydrodynamics, edited by D. B. Spalding (Advance, London, 1977), p.65.

[3] P. A. Monkewitz, Eur. J. Mech. B **9**, 395 (1990).

[4] D. J. Tritton, *Physical Fluid Dynamics* (Oxford Univ. Press, Oxford, 1988).

[5] H. W. Müller, M. Lücke, and M. Kamps, Europhys. Lett. **10**, 451 (1989); Phys. Rev. A **45**, 3714 (1992).

[6] H. W. Müller, M. Tveitereid, and S. Trainoff, Phys. Rev. E **48**, 263 (1993).

[7] M. T.Ouazzani, J. K. Platten, and A. Mojtabi, Int. J. Heat Mass Transfer **33**, 1417 (1990).

[8] H. R. Brand, R. J. Deissler, and G. Ahlers, Phys. Rev. A **43**, 4262 (1991).

[9] J. M. Luijkx and J. K. Platten, Int. J. Heat Mass Transfer **24**, 1287 (1981).

[10] J. M. Luijkx, Ph.D. thesis, University of Mons (Belgium), 1983 (unpublished).

[11] B. S. Ng and E. R. Turner, Proc. R. Soc. London Ser. A **382**, 83 (1982).

[12] M. T. Ouazzani, J. P. Platten, A. Mojtabi, H. W. Müller, and M. Lücke (unpublished).

[13] H. A. Snyder, Proc. R. Soc. London Ser. A **265** 198 (1962).

[14] K. L. Babcock, G. Ahlers, and D. S. Cannell, Phys. Rev. Lett. **24**, 3388 (1991); Physica D **61**, 40 (1992). They used $\epsilon_{\mathrm{BAC}} = \frac{\Omega}{\Omega_c(Re=0)} - 1 = \sqrt{1+\epsilon} - 1$ as a control parameter. Thus our τ_0, ξ_0^2 are twice as large as theirs and $\epsilon_c \simeq 2\epsilon_{\mathrm{BAC}}^c$.

[15] T. Tsameret and V. Steinberg, Europhys. Lett. **14**, 331 (1991); Phys. Rev. Lett. **67**, 3392 (1991).

[16] T. Tsameret and V. Steinberg (unpublished).

[17] K. Bühler, Strömungsmechanik und Strömungsmachinen, **35** (1982); Z. Angew. Math. Mech. **64**, 180 (1984).

[18] K. Bühler and F. Polifke, in *Nonlinear Evolution of Spatio-temporal Structures in Dissipative Continuous Systems*, edited by F. Busse and L. Kramer (Plenum Press, New York, 1990), p.21.

[19] D. I. Takeuchi and D. F. Jankowski, J. Fluid Mech. **102**, 101 (1981). In order to compare with our results one has to use the relation $T = \eta/(1-\eta)T_{\mathrm{TJ}}^2$ between our and their Taylor number.

[20] R.M. Lueptow, A. Docter, and K. Min, Phys. Fluids A **4**, 2446 (1992).

[21] R. J. Deissler, Physica D **25**, 233 (1987); J. Stat. Phys. **54**, 1459 (1989).

[22] R. Tagg, W.S. Edwards, and H. L. Swinney, Phys. Rev. A **42**, 831 (1990).

[23] M. Lücke and A. Recktenwald, Europhys. Lett. **22**, 559 (1993).

[24] A. Bers, in *Basic Plasma Physics I*, edited by A. A. Galeev and R. N. Sudan (North-Holland, New York, 1983).

[25] R. J. Briggs, *Electron Stream Interaction with Plasmas* (MIT Press, Cambridge, MA, 1964).

[26] L. D. Landau and E. M. Lifshitz, *Physical Kinetics* (Pergamon Press, New York, 1981), Vol. 10.

[27] P. Büchel, *Diplomarbeit*, Universität des Saarlandes, 1992 (unpublished).

[28] A review of the Couette-Taylor system without throughflow is given by R. C. DiPrima and H. L.Swinney, in *Hydrodynamic Instabilities and Transitions to Turbulence*, edited by H. L. Swinney and J. P. Gollub (Springer, Berlin, 1981), p. 139.

[29] A. C. Newell and J. A. Whitehead, J. Fluid Mech. **38**, 279 (1969).

[30] L. A. Segel, J. Fluid Mech. **38**, 203 (1969).

[31] R. Graham and J. A. Domaradzki, Phys. Rev. A **26**, 1572 (1982).

[32] H. Yahata, Prog. Theor. Phys. **57**, 347 (1977).

[33] S. Goldstein, Proc. Cambridge Philos. Soc. **33**, 41 (1937).

[34] R. J. Cornish, Proc. R. Soc. London Ser. A **140**, 227 (1933).

[35] A. Fage, Proc. R. Soc. London Ser. A **165**, 501 (1938).

[36] S. Chandrasekhar, Proc. Natl. Acad. Sci. USA **46**, 141 (1960).

[37] S. Chandrasekhar, Proc. R. Soc. London Ser. A **265**, 188 (1962).

[38] R. C. DiPrima, J. Fluid. Mech. **9**, 621 (1960).

[39] S. K. Datta, J. Fluid. Mech. **21**, 635 (1965).

[40] L. Elliott, Phys. Fluids **16**, 577 (1973).

[41] T. H. Hughes and W. H. Reid, Philos. Trans. R. Soc. London Ser. A **263**, 57 (1968).

[42] M. A. Hasoon and B. W. Martin, Proc. R. Soc. London Ser. A **352**, 351 (1977). For comparison of T_c see [19].

[43] R. C. DiPrima and A. Pridor, Proc. R. Soc. London Ser. A **366**, 555 (1979).

[44] K. C. Chung and K. N. Astill, J. Fluid Mech. **81**, 641 (1977). For comparison of T_c see comparison in Ref. [19].

[45] K. W. Schwarz, B. E. Springett, and R. J. Donnelly, J. Fluid Mech. **20**, 281 (1964).

[46] H. M. Nagib, Ph.D. thesis, Department of Mechanical and Aerospace Engineering, Illinois Institute of Technology, 1972 (unpublished).

[47] J. A. Mavec, M.S. thesis, Department of Mechanical and Aerospace Engineering, Illinois Institute of Technology, 1973 (unpublished).

[48] N. Gravas and B. W. Martin, J. Fluid Mech. **86**, 385 (1978).

[49] S. Chandrasekhar, *Hydrodynamic and Hydromagnetic Stability* (Dover, New York, 1981).

[50] R. J. Donnelly, K. W. Schwarz, and P. H. Roberts, Proc. R. Soc. London Ser. A **283**, 550 (1965).

[51] C. A. Jones, J. Fluid Mech. **157**, 135 (1985).

[52] W. F. Langford, R. Tagg, E. Kostelich, H. L. Swinney, and M. Golubitsky, Phys. Fluids **31**, 776 (1988).

[53] J. Stoer and R. Bulirsch, *Numerische Mathematik 2* (Springer, Berlin, 1990).

[54] W. H. Press, B. P. Flannery, S. A. Teukolsky, and W. T. Vetterling, *The Art of Scientific Computing. Numerical Recipes in Fortran* (Cambridge University Press, Cambridge, England, 1987).

[55] E. R. Krueger, A. Gross, and R. C. DiPrima, J. Fluid Mech. **24**, 521 (1966).

[56] M. A. Dominguez-Lerma, G. Ahlers, and D. S. Cannell, Phys. Fluids **27**, 856 (1984). In order to compare with our results one has to use the relation $T = \frac{1+\eta}{2\eta} T_{\mathrm{DLAC}}$ between the Taylor numbers.

[57] A. C. Newell, Lect. Appl. Math. **15**, 157 (1974); in *Pattern Formation by Dynamic Systems and Pattern Recognition*, Proceedings of the International Symposium on Synergetics, Bavaria, 1979, edited by H. Haken (Springer, New York, 1979); in *Propagation in Systems far from Equilibrium*, edited by J. E. Wesfreid, H. R. Brand, P. Manneville, G. Albinet, and N. Boccara (Springer, Berlin, 1988).

[58] P. Huerre and P. A. Monkewitz, J. Fluid. Mech. **150**, 151 (1985).

[59] C. M. Bender and S. A. Orszag, *Advanced Mathematical Methods for Scientists and Engineers* (McGraw-Hill, New York, 1978).

[60] A. Davey, J. Fluid. Mech. **14**, 336 (1962).

[61] M. Lücke and D. Roth Z. Phys. B **78**, 147 (1990). They used $\epsilon_{\mathrm{LR}} = \frac{\Omega}{\Omega_c} - 1$ as control parameter.

[62] D. Roth (private communication).

[63] K. L. Babcock (private communication).